Effect of natural carbonation on chloride binding behaviours in OPC paste investigated by a thermodynamic model

Guo, Bingbing; Qiao, Guofu; Han, Peng; Li, Zhenming; Fu, Qiang

DOI
10.1016/j.jobe.2022.104021

Publication date
2022

Document Version
Final published version

Published in
Journal of Building Engineering

Citation (APA)
Guo, B., Qiao, G., Han, P., Li, Z., & Fu, Q. (2022). Effect of natural carbonation on chloride binding behaviours in OPC paste investigated by a thermodynamic model. *Journal of Building Engineering*, *49*, Article 104021. https://doi.org/10.1016/j.jobe.2022.104021

Journal of Building Engineering 49 (2022) 104021

Contents lists available at ScienceDirect

Journal of Building Engineering

journal homepage: www.elsevier.com/locate/jobe

Effect of natural carbonation on chloride binding behaviours in OPC paste investigated by a thermodynamic model

Bingbing Guo [a], Guofu Qiao [b,*], Peng Han [b], Zhenming Li [c,**], Qiang Fu [a]

[a] School of Civil Engineering/Key Lab of Engineering Structural Safety and Durability, Xi'an University of Architecture and Technology/State Key Laboratory of Green Building in Western China, Xi'an, 710055, China
[b] School of Civil Engineering, Harbin Institute of Technology, Harbin, 150090, China
[c] Department of Materials and Environment (Microlab), Faculty of Civil Engineering and Geoscience, Delft University of Technology, Delft, 2628, CN, the Netherlands

ARTICLE INFO

Keywords:
Cement-based materials
Carbonation
Chloride binding
Thermodynamic modelling

ABSTRACT

The combined effects of carbonation and chloride attack can accelerate the degradation of reinforced concrete (RC) structures. In this study, the effect of natural carbonation on the chloride binding behaviours in Ordinary Portland cement (OPC) paste was investigated. The phase-equilibrium model for the dissolution/precipitation reactions and the surface complexation model for the ionic adsorption of C–S–H were adopted. An experiment from the literature was used as the benchmark. The results indicate that Kuzel's salt is produced when OPC paste is exposed to a mild chloride attack. During the natural carbonation process, Kuzel's salt is converted into Friedel's salt. As the carbonation continues, the Friedel's salt disappears. Complete natural carbonation results in a total loss of chemical binding capacity, and only a partial loss of the physical binding capacity in cement-based materials. This completely differs from the accelerated carbonation commonly used in the laboratory, which can cause complete loss of both chemical and physical binding capacity. Therefore, the durability design of RC structures vulnerable to the combined attack of chloride and carbonation based on the results of the accelerated carbonation is conservative.

1. Introduction

Reinforced concrete (RC) structures are commonly used in various civil engineering applications. However, the corrosion of reinforcing steel induced by chloride attack, which commonly occurs in marine environments or locations where de-icing salts are used, is one of the primary factors contributing to the deterioration of the durability of RC structures [1,2]. Normally, the high alkalinity of a typical concrete pore solution results in a passive protective film against corrosion at the steel surface. However, when a sufficient amount of chloride penetrates the concrete down to the steel surface, the passive film is destroyed [3–5]. At this point, the presence of both moisture and oxygen initiates corrosion of the reinforcing steel. Corrosion can reduce the effective cross-sectional area of the reinforcing steel, which causes a decrease in the bearing capacity of RC structures, and even structural collapse [6–8].

When chloride penetrates cement-based materials, chemical binding occurs, in which some chlorides chemically react with cement

* Corresponding author.
** Corresponding author.
E-mail addresses: guobingbing212@163.com (B. Guo), qgf_forever@hit.edu.cn (G. Qiao), han_hiter@163.com (P. Han), Z.li-2@tudelft.nl (Z. Li), fuqiangcsu@163.com (Q. Fu).

https://doi.org/10.1016/j.jobe.2022.104021
Received 19 April 2021; Received in revised form 14 July 2021; Accepted 7 January 2022
Available online 11 January 2022

hydrates (primarily the AFm phase) [9–11]. Physical binding also occurs, in which some chlorides physically bind to the surface of the hydrate phase because of the ionic binding properties of its surface groups [12–16]. The remaining chlorides exist in the pore solution as free ions. Chloride binding retards the penetration ability of the chloride and delays the initiation of corrosion [10,17–21]. Thus, the chloride binding capacity of cement-based materials directly affects the durability of RC structures [22–27].

Concrete carbonation is another primary mechanism for the corrosion of reinforcing steel [28–34]. The rapid development of the global economy has resulted in rising the atmospheric CO_2 concentration. In 2011, the atmospheric CO_2 concentration was 391 ppm, which exceeded the pre-industrial levels by approximately 40% [35]. As reported by Stewart et al. [36], the corrosion damage risks due to carbonation may exceed 16% by the year 2100. This means that at least one in six RC structures will suffer from carbonation-induced corrosion damage. Thus, the degradation of the durability of RC structures caused by carbonation will become a serious concern. Concrete carbonation can decrease the pH of the pore solution, jeopardizing the reinforcing steel [37,38]. In addition, carbonation also lowers the chloride binding capacity of cement-based materials owing to the decalcification or dissolution of the cement hydrates, which has already been confirmed by the experimental results reported in Refs. [29,39–49]. The combined effects of carbonation and chloride attack accelerate the initiation of corrosion of the reinforcing steel, especially in RC structures exposed to marine atmospheric environments.

Experiments to conduct the natural carbonation of cement-based materials need to take several years, or even decades. To shorten the experimental period, higher CO_2 concentrations in most of investigations were used to study the effect of carbonation on the chloride binding capacity. However, Castellote et al. [50], in their investigation on the chemical changes and phases of hardened cement pastes carbonated at different CO_2 concentrations (i.e., 3%, 10%, and 100%), found that C–S–H completely disappeared when the cement pastes were subjected to CO_2 concentrations of 10% and 100%, whereas the Ca/Si ratio of C–S–H decreased when the cement pastes were subjected to natural carbonation and 3% CO_2 concentration. An experimental study performed by Groves et al. [51], found that the structure of a hardened C_3S cement paste fully carbonated in pure CO_2 gas differed from that subjected to natural carbonation. Anstice et al. [52] also found that the pore solution, mineralogy and pore structure of fully carbonated cement-based materials with different CO_2 concentrations were significantly different. All these results indicate that natural carbonation in cement-based materials is completely different from accelerated carbonation [37,50–53].

However, investigations on the effect of natural carbonation on the chloride binding behaviour have seldom been reported, partially because of the long period required for experiments. With the rapid development of thermodynamic database for cement-based materials [54–58], thermodynamic modelling has become an invaluable tool in addition to experimental approaches for studying the durability of cement-based materials subjected to chemical reactions [54,59–62]. The natural carbonation of cement-based materials is essentially the result of a series of complicated chemical reactions between atmospheric CO_2 (g), the pore solution, and cement hydrates, while the chloride binding is the result of physical and chemical reactions between the pore solution and the cement hydrates. Therefore, in this study, the phase-equilibrium model for the dissolution/precipitation reactions and the surface complexation model for the ionic adsorption of C–S–H are used to investigate the effect of natural carbonation on chloride binding in cement-based materials. The detailed theoretical background is presented in the next section.

2. Theoretical background

Elakneswaran et al. [12,59] and Hirao et al. [16] found that the physical binding of chloride in cement-based materials is dominated by C–S–H, and that the physical binding of other hydrate phases (such as portlandite, ettringite and AFm) can be neglected. The physical binding of C–S–H for chloride was successfully predicted by the surface complexation model in the investigations of Elakneswaran et al. [12,59]. Thus, in this study, the physical binding in cement-based materials is assumed to be the result of the surface complexation reactions of C–S–H for the free ions in the pore solution. In addition, the products of chemical binding, including Kuzel's salt ($C_3A{\cdot}0.5CaCl_2{\cdot}0.5CaSO_4{\cdot}10H_2O$) [9,10] and Friedel's salt ($C_3A{\cdot}CaCl_2{\cdot}10H_2O$) [9,11,19,21], are considered. The formations of Kuzel's salt and Friedel's salt are assumed to result from the precipitation reactions of some species in the pore solution, such as Cl^-, Ca^{2+}, SO2- 4, AlO- 2 and H_2O. This leads to the dissolution of other hydrate phases, especially the AFm phase [54]. As previously mentioned, carbonation is the result of the chemical reactions between CO_2 (g), the pore solution, and cement hydrates. In the study, it is assumed that the carbonation process is as follows: CO_2 gas from the external atmosphere dissolves into the pore solution, and exists in the form of HCO_3^-. HCO_3^-, OH^-, and Ca^{2+} precipitate into $CaCO_3$. The continuous consumption of Ca^{2+} leads to the decalcification or dissolution of the hydrate phases, while the consumption of OH^- results in a decrease in the pH of the pore solution. Furthermore, the decalcification or dissolution of the hydrate phases leads to a decrease in the chloride binding capacity of cement-based materials.

According to Henry's law (q. (1)), the amount of atmospheric CO_2 that dissolves into the concrete pore solution is proportional to its partial pressure [31],

$$m_{CO_2} = H_{CO_2} p_{CO_2} \tag{1}$$

where m_{CO2} is the molar concentration of CO_2 dissolved in an aqueous solution (mol/kg), and p_{CO2} is the partial pressure of CO_2 in the air (kPa). The CO_2 concentration in air in 2011 was 0.039% [35]. Thus, 39 Pa was adopted as the partial pressure value in this study. H_{CO2} is Henry's law constant for CO_2, and has the value of 3.39×10^{-4} mol/kg·kPa under standard atmospheric pressure and temperature (25 °C) [63].

When CO_2 in the gas phase dissolves into the pore solution, or when chloride enters a cement-based material, the existing thermodynamic equilibrium between the pore solution and the cement hydrates is broken, and a new thermodynamic equilibrium is established based on the dissolution/precipitation and surface complexation reactions between the pore solution and the cement hydrates.

Nearly all the dissolution/precipitation reactions in cement hydrates and their equilibrium constants are listed in Cemdata18 [54], and will not be presented here. The phase-equilibrium model (Eq. (2)) is used to describe the dissolution/precipitation reactions via the law of mass action (LAM) [59]:

$$K_p = \prod_m (\gamma_m c_m)^{n_{m,p}} \tag{2}$$

where K_p is the equilibrium constant of the dissolution and precipitation reactions between the hydrate phase p and the pore solution; γ_m and c_m respectively denote the activity coefficient and concentration of ion m involved in the associated reaction, and $n_{m,p}$ denotes the stoichiometric coefficient of ion m.

Additionally, the WATEQ Debye-Huckel activity equation (Eq. (3)) is used for the activity coefficient γ_m of ion m:

$$\log(\gamma_m) = \frac{-Az_m^2\sqrt{\mu}}{1 + Ba_m\sqrt{\mu}} + b_m\mu \tag{3}$$

where A and B are constants dependent only on the temperature; z_m is the valence of ion m; a_m and b_m are the ion-specific parameters from the mean-salt activity-coefficient data, given in Cemdata18 [54]; μ is the ionic strength of the aqueous solution (mol/L), and is defined as Eq. (4):

$$\mu = 0.5\sum_{m=1}^{J} z_m^2 c_m \tag{4}$$

where J represents the number of species in the pore solution, and includes free species such as K^+, Na^+, Ca^{2+}, OH^-, Cl^-, and SO_4^{2-}, as well as aqueous complexes such as $Al(OH)_4^-$ and $CaOH^+$.

Because there are many silanol sites (≡SiOH) and silandiol sites (≡Si$(OH)_2$) on the C–S–H surface [15], the ionization, proton migration and surface site reactions occur when C–S–H comes into contact with an aqueous solution. Elakneswaran et al. [12,59] and Tran et al. [64] reported that the surface reactions between the silandiol sites of C–S–H and aqueous solution can be neglected. Thus, the free ions in the pore solution are assumed to react only with the surface silanol sites of C–S–H in this study. The primary surface site reactions between C–S–H and the free ions are presented in Table 1. Similarly, the surface site reactions can be described by the LAM (Eq. (5)) [59]:

$$K_i = \left(\prod_m (\gamma_m c_m)^{n_{m,i}}\right)\exp\left(\frac{F\psi_0}{RT}\Delta z_i\right) \tag{5}$$

where K_i denotes the equilibrium constant of the adsorption reaction of ion i onto the surface layer, and is given in Table 1; F is the Faraday constant (96,485 C/mol); R is the universal gas constant (8.314 J/(K·mol)); T is the absolute temperature (K); ψ_0 is the surface potential; Δz_i is the net change in surface charge due to the formation of the surface species.

According to the theory of the Gouy-Chapman diffuse layer [20], the surface charge density σ and the surface potential ψ_0 (V) are related by Eq. (6):

$$\sigma = -(8000RT\varepsilon\varepsilon_0 m)^{\frac{1}{2}}\sinh\left(\frac{zF\psi_0}{2RT}\right) \tag{6}$$

where ε is the relative permittivity of water ($\varepsilon = 78.5$, at 25 °C); ε_0 is the permittivity of free space (8.854×10^{-12} F/m); m is the molar electrolyte concentration (mol/L); z is the valence of the symmetrical electrolyte.

Carbonation can change the components of the hydrate phases in cement-based materials and the Si/Ca ratio of the C–S–H phase, and thus affecting the chloride binding capacity of cement-based materials. The carbonation reactions in cement-based materials are governed by Eqs. (1)–(4), while the physical and chemical binding of chloride is described using Eqs. (2)–(6).

3. Thermodynamic modelling

It is well known that the relative humidity of the environment and the saturation degree of concrete affect primarily the carbonation rate, but have little effect on the carbonation reaction mechanism. Hence, the natural carbonation in this study was assumed to occur under a fixed CO_2 concentration (0.039%), which corresponded to the natural conditions of the atmosphere. The

Table 1
Adsorption reactions of C–S–H for free ions and their equilibrium constants at 25 °C.

Primary site reactions	Log K_p
≡SiOH + OH^- → ≡SiO^- + H_2O	−12.7 [59]
≡SiOH + Ca^{2+} → ≡$SiOCa^+$ + H^+	−9.4 [59]
≡SiOH + Cl^- → ≡SiOHCl^-	−0.35 [59]
≡SiOH + Na^+ → ≡SiONa + H^+	−13.6 [59]
≡SiOH + K^+ → ≡SiOK + H^+	−13.6 [59]

specimen was assumed to be fully saturated.

Ordinary Portland cement (OPC), the most widely used type of cement, was chosen for this study. Saillio et al. [48] studied the chloride binding in sound and carbonated cement-based materials. Their experiment was taken as the benchmark example in this study to investigate the effect of natural carbonation on chloride binding in cement. The main constituents of the cement used were CaO (62.53%), SiO_2 (19.54%), Al_2O_3 (4.98%), Fe_2O_3 (2.90%), MgO (0.84%), SO_3 (2.97%), K_2O (0.82%), Na_2O (0.30%) and CO_2 (1.92%), with a water/cement ratio of 0.50 [48]. The specimens were cured over a period of 90 days or 1 year in Ref. [48]. To reduce the effect of age on the evolution of the phase assemblages, the specimens cured over a period of 1 year were selected for this study. The phase assemblages of the cement hydrates and pore solution in the paste were then calculated using the thermodynamic model. For the C–S–H phase, a CSH3T model based on an ideal solid solution was used. The solid solution consisted of $C_3S_2H_5$ (Ca/Si = 1.5), $C_{2.5}S_{2.5}H_5$ (Ca/Si = 1) and $C_2S_3H_5$ (Ca/Si = 0.6667) [65]. Tables 2 and 3 present the calculation results for 1 kg of cement. The results show that the phase assemblages consisted of C–S–H with a 1.5 Ca/Si ratio, portlandite, ettringite, monosulfate and monocarbonate; the weight of the pore solution was 0.141 kg, and the primary free ions were Na^+, K^+, Ca^{2+}, and OH^-. The values in Tables 2 and 3 were used as the initial material parameters. To simulate the degradation of OPC paste subjected to different degrees of chloride attack, various amounts of NaCl were added to the pore solution. The specific surface area of C–S–H (m^2/g) is 500 m^2/g [15]. During carbonation, the decalcification of C–S–H affects the number of surface silanol. The following formula (Eq. (7)) [66] is used for the solid solution:

$$Ca_xH_{2(n+1-x)}Si_nO_{(3n+1)} \cdot mH_2O \tag{7}$$

Here, $2(n+1\text{-}x)$ is the number of surface silanols, which is determined by the amounts of Ca and Si in the C–S–H phases. When $x = 0$, C–S–H is assumed to take the form of amorphous silica, which cannot bind any chloride ions because of the decalcification caused by carbonation. The PHREEQC COM module [67,68] in MATLAB was developed to solve the thermodynamic model.

4. Results

4.1. Chloride binding in CO_2-free environment

The chloride binding of the cement hydrates, that is the amounts of chloride bound by C–S–H, Friedel's salt and Kuzel's salt, at various NaCl concentrations was predicted using the thermodynamic model. The results are shown in Fig. 1. Owing to the surface charge, C–S–H can bind free ions from the pore solution [12,13,15,69]. As the free chloride concentration in the pore solution increases, the amount of chloride physically bound by C–S–H increases. This increasing trend is prominent at lower free chloride concentration. The chloride binding behaviours under different environmental conditions have already been discussed in our previous paper [70], in which Kuzel's salt was not considered in the chemical binding. Thus, the results related to chemical binding are explained in detail here.

The AFm family consists of primarily monosulfate, hydroxy-AFm and monocarbonate in cementitious materials [9,71]. Both Kuzel's salt and Friedel's salt are the products of chemical reactions between AFm and free chloride, and have been identified as chloro-sulfoaluminate and chloroaluminate AFm phases, respectively [9,10,19,21]. The results predicted by the thermodynamic model indicate that Kuzel's salt begins to produce when the free chloride concentration is approximately 0.819 mol/L. As the free chloride concentration increases, the amount of Kuzel's salt will increase up to a maximum value and then remain at that value until Friedel's salt is produced. With the formation of Friedel's salt, the amount of Kuzel's salt begins to decrease until it disappears. By studying the stability and solubility of the AFm phases, Glasser et al. [9] and Balonis et al. [72] postulated that the formation of Kuzel's salt occurs in a low chloride concentration environment. The X-ray powder diffraction (XRD) results of Zibara [27] also indicated that AFm can be converted to Kuzel's salt at a low chloride concentration, and can again be converted to Friedel's salt when the chloride concentration increases. It was found in Ref. [73] that Kuzel's salt was produced when 25 g of paste in equilibrium with 3 mol/L of NaCl solution was exposed to saturated $Ca(OH)_2$ solution. Thus, both the results predicted by the thermodynamic model and those obtained from experiments [9,27,72,73] indicate that Kuzel's salt can be produced when cement-based materials are exposed to a mild chloride attack.

In addition, monosulfate reacts with chloride ions, which replace the sulfate. Simultaneously, sulfate can react with part of the monosulfate, producing ettringite. Thus, the formation of Kuzel's salt or Friedel's salt increases the amount of ettringite, as shown in Fig. 1. As the free chloride concentration increase continuously, moncarbonate begins to react with chloride ions to produce Friedel's salt. Compared to monosulfate, moncarbonate is more stable, and therefore, monosulfate reacts with chloride ions more easily.

The total amount of chemically and physically bound chloride as a function of the free chloride concentration*, which is called the chloride binding isotherms (CBIs),* is polted in Fig. 2. *As* the free chloride concentration *increases*, the total bound chloride *increases with a gradually decay in the increase rate*. In the experiment by Saillio et al. [48], the total chloride bound by the OPC paste at different NaCl concentrations was measured, and the results are shown in Fig. 2. The thermodynamic model slightly overestimates the chloride binding capacity of cement-based materials, and the error decreases with increasing free chloride concentration. Therefore, the thermodynamic model can predict the chloride binding capacity of cement-based materials to some extent.

According to the results in Figs. 1 and 2, the chloride binding can be divided into four stages as the free chloride concentration

Table 2
Phase assemblages of the cement hydrates.

Phase	C–S–H	Portlandite	Ettringite	Monosulfate	Monocarbonate
Content (mol/1 kg of cement)	3.25	4.13	0.07	0.023	0.019

Table 3
Primary ions of the pore solution.

Ion	Na^+ (mM)	K^+ (mM)	Ca^{2+} (mM)	SO_4^{2-}	pH
Content	48.36	202.72	0.42	0.30	13.55

The weight of the pore solution was 0.141 kg for 1 kg of initial cement.

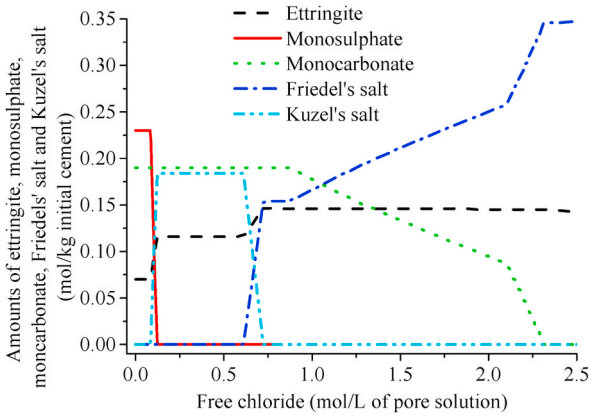

Fig. 1. Chemically bound chloride in cement-based materials.

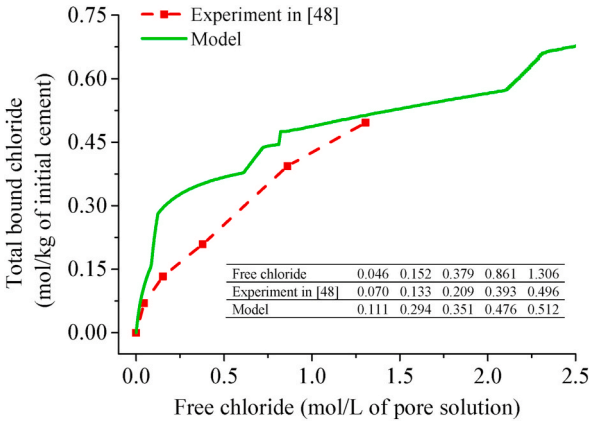

Fig. 2. Comparison of chloride binding isotherms in CO_2-free environment as measured by Saillio et al. [48] and predicted by the thermodynamic model.

increases. The first stage is the binding reactions of C–S–H. The second stage is the coexistence of the binding reactions of C–S–H and the formation of Kuzel's salt. The third stage is the coexistence of the binding reactions of C–S–H and the simultaneous formation of Kuzel's salt and Friedel's salt. The fourth stage is the coexistence of the binding reactions of C–S–H and the formation of Friedel's salt. These four stages represent the typical chloride binding behaviours in cement-based materials under varying degrees of chloride attack. From the thermodynamic insight, owing to the penetration of the chloride, a new equilibrium between pore solution and cement hydrate is continuously established via dissolution/precipitation and surface complexation reactions. However, the amount of chloride physically and chemically bound by the cement hydrates is limited because the C–S–H and AFm contents in the cement hydrates are fixed.

4.2. Effect of natural carbonation on chloride binding

To understand the effect of natural carbonation on chloride binding, the pH of the pore solution and the phase assemblages in the OPC paste as functions of the carbonation degree were predicted using the thermodynamic model. The results are shown in Figs. 3 and 4. Note that the abscissa in Fig. 3 is the amount of CO_2 absorbed by the hydrate products in 1 kg of cement. It can be seen that the amount of absorbed CO_2 is 9.82 mol when the paste resulting from 1 kg of cement is completely carbonated. At this point, the carbonation degree is 1.0. The carbonation degree is used in the following related figures.

Natural carbonation can lower the pH of pore solution. The change in the pH of the pore solution is closely related to the carbonation reactions of the hydrate phases. When portlandite is completely carbonated, the pH decreases slightly from 13.56 to

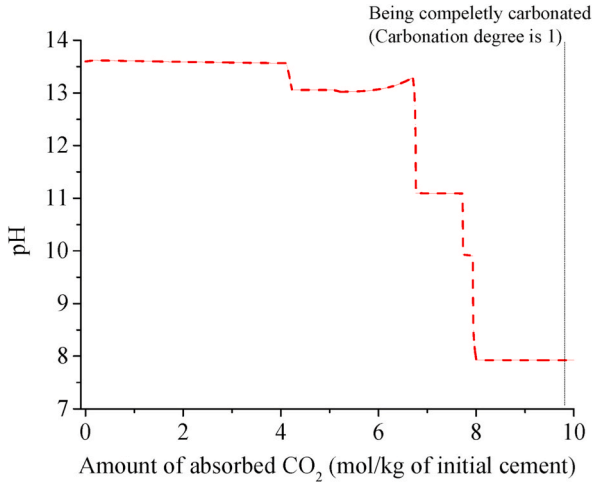

Fig. 3. pH value during the carbonation process.

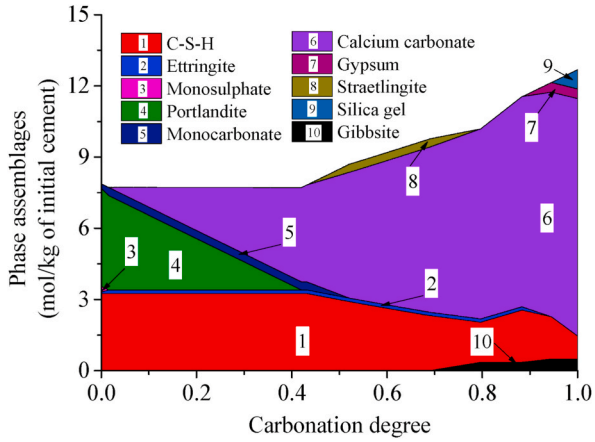

Fig. 4. Phase assemblages in the paste as a function of the carbonation degree.

13.06. With the decalcification of C–S–H, the pH decreases remarkably.

As shown in Fig. 4, monosulfate is the most easily carbonated among all the hydrate phases. As the carbonation degree increases, calcium carbonate, straetlingite, gypsum, silica gel and gibbsite are successively produced, and monosulfate, portlandite, monocarbonate, straetlingite and ettringite successively disappear. Among them, straetlingite is an intermediate product [74,75]. The phase assemblages of the OPC paste subjected to a complete carbonation consist of C–S–H with a lower Ca/Si ratio, gypsum, calcium carbonate, gibbsite and silica gel.

Based on the results in section 4.1, four different free chloride concentrations (0.05 mol/L, 0.40 mol/L, 0.67 mol/L and 1.0 mol/L) were chosen to represent the four kinds of typical chloride binding behaviours with varying degrees of chloride attack. Note that only the physical binding of chloride occurs without any chemical binding when the free chloride concentration is 0.05 mol/L, which can also be seen from Fig. 1. Thus, Fig. 5 illustrates the effect of natural carbonation on the chemical binding of chloride in the latter three situations where the free chloride concentrations are 0.40 mol/L, 0.67 mol/L, and 1.0 mol/L. As shown in Fig. 5 (a) and (b), the amount of Friedel's salt increases with the degree of carbonation until it reaches a maximum. This is accompanied by a decrease in the amount of Kuzel's salt, which continues until Kuzel's salt disappears. This phenomenon indicates that natural carbonation leads to the conversion of Kuzel's salt into Friedel's salt. With the continuous increase in the degree of carbonation, the hydrate phases containing aluminum changes into straetlingite (Fig. 4). This causes Friedel's salt to disappear. Suryavanshi et al. [40] also found that natural carbonation could cause the disappearance of Friedel's salt. The experimental results of Saillio et al. [48] indicated that carbonation at the CO_2 concentration of 1.5% could lead to the complete dissolution of Friedel's salt. Goni and Guerrero [39] found that Friedel's salt completely decomposed after six days of carbonation at 5% CO_2 concentration. In the investigations of Geng et al. [41] and Chang et al. [47,76], carbonation at the CO_2 concentration of 20% caused Friedel's salt to completely disappear. It is therefore concluded that both natural and accelerated carbonation can lead to a complete loss of the chemical binding capacity in cement hydrates.

Fig. 6 shows the effect of natural carbonation on the physical binding of chloride. To facilitate the illustration to this effect, the Ca/

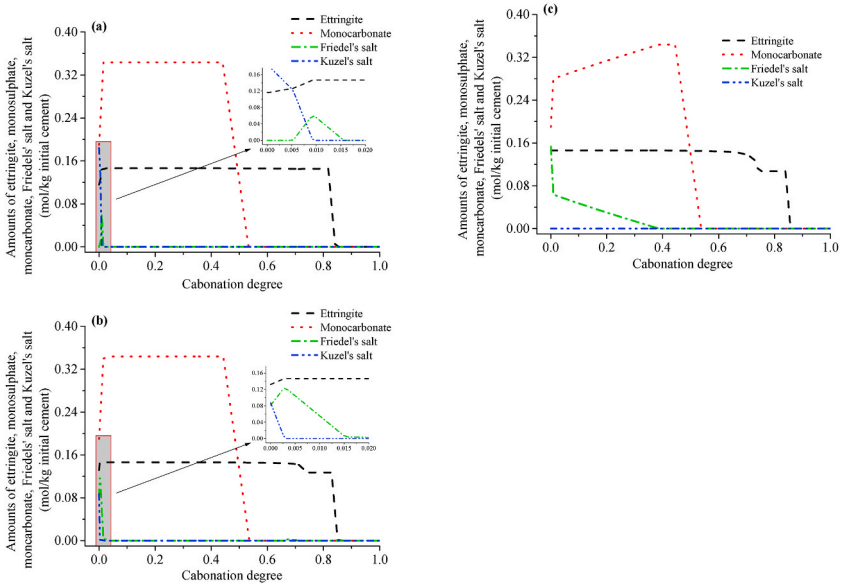

Fig. 5. Effect of carbonation degree on the amounts of Friedel's and Kuzel's salt at the free chloride concentrations of (a) 0.40 mol/L, (b) 0.67 mol/L, and (c) 1.0 mol/L in the pore solution.

Si ratio in the C–S–H phases at different degrees of carbonation are also shown. At low degrees of carbonation, the amount of chloride bound by C–S–H in the four cases display a significant increasing trend, except at the free chloride concentration of 0.05 mol/L. Combining this with the results shown in Figs. 1 and 2, it can be seen that this increase is due to the carbonation reaction of Kuzel's salt. The dissolution of Kuzel's salt not only promotes the formation of Friedel's salt, but also contributes to the physical binding of C–S–H.

As the degree of carbonation continues to increase, there is an evident decrease in the amount of physically bound chloride when the decalcification of C–S–H begins to occur at the carbonation degree of 0.51, especially at the free chloride concentrations of 0.40

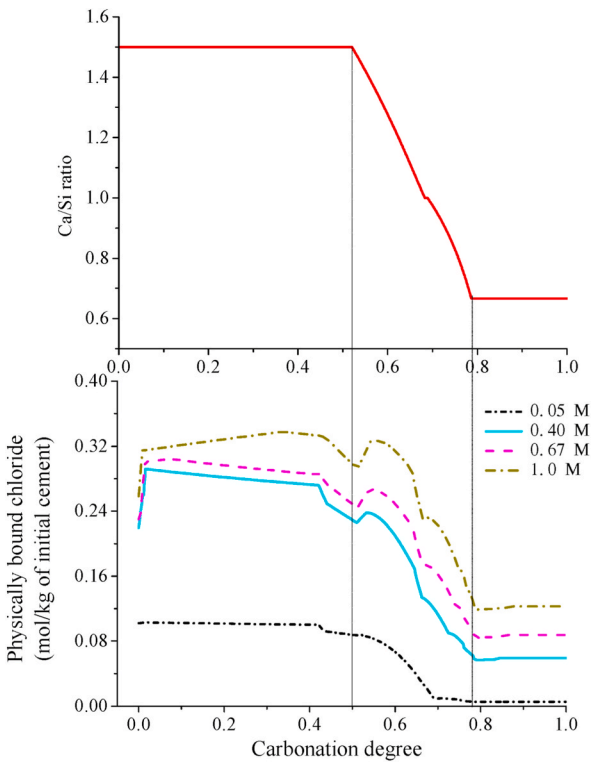

Fig. 6. Ca/Si ratio of C–S–H and its physical binding for chloride as functions of the carbonation degree.

mol/L, 0.67 mol/L and 1.0 mol/L. The Ca/Si ratio of C–S–H directly affects the number of surface silanols. Thus, the decrease in the Ca/Si ratio caused by carbonation leads to a decrease in the physical binding capacity of C–S–H. A similar result was found for accelerated carbonation, as reported in Refs. [41,47,48,76]. However, owing to the existence of C–S–H with a low Ca/Si ratio, some chlorides are still physically bound. This means that cement-based materials that have undergone a complete natural carbonation still retain a portion of the physical binding capacity, which differs from the result that accelerated carbonation can lead to complete loss of chloride binding capacity reported in Refs. [41,47,48,76].

4.3. Effect of CO_2 concentration on chloride binding isotherms (CBIs)

The chloride binding isotherms (CBIs) of the completely carbonated cement-based materials at different CO_2 concentrations were predicted using the thermodynamic model, and shown in Fig. 7. There are significant differences in the CBIs at different concentrations of CO_2 used to carbonate the paste. As the CO_2 concentration increases, the amount of bound chloride decreases. As described in Section 4.2, a paste that has undergone complete natural carbonation completely loses its chemical binding capacity, and retains only a portion of its physical binding capacity. Increasing the CO_2 concentration causes more severe decalcification of C–S–H, and even total decalcification [50,53]. Thus, as the CO_2 concentration increases, the physical binding capacity of completely carbonated cement-based material gradually decreases until it is completely lost. In the experiment performed by Saillio et al. [48], a CO_2 concentration of 1.5% was used to carbonate the paste, and the CBIs were measured. Their results are also presented in Fig. 7. The completely carbonated paste at this CO_2 concentration completely lost both its physical and chemical chloride binding capacity in line with the results predicted by the thermodynamic model.

The phase assemblages in the paste as a function of the carbonation degree at 1.5% CO_2 concentration were also predicted, and the results are shown in Fig. 8. It is clear that the C–S–H phases will be completely decalcified when the OPC paste is subjected to carbonation at such a high CO_2 concentration, which differs from the natural carbonation shown in Fig. 4. This is also the reason why the completely carbonated paste at 1.5% CO_2 concentration completely loses its chloride binding capacity.

5. Discussion

The carbonation of cement-based materials causes a decrease in the pH of the pore solution, and the dissolution of the hydrate phases (see Figs. 4 and 8). The pH does not decrease significantly before portlandite is completely carbonated. However, a remarkable drop in pH can be seen when significant decalcification of the C–S–H phases occurs. The pH can be reduced to a neutral value of nearly 7.9 when cement-based materials are subjected to a complete natural carbonation. In the laboratory, a high CO_2 concentration is commonly used to accelerate the carbonation of cement-based materials. The results in Figs. 4 and 8 illustrate that the difference between natural carbonation and accelerated carbonation is the decalcification of C–S–H. At higher CO_2 concentrations, the C–S–H phases will experience more severe decalcification [50], which leads to a decrease in the ability to physically bind chloride in cement-based materials. This is also the reason why the effects of natural and accelerated carbonation on CBIs are different.

The losses in the physical binding capacity of cement-based materials in the four cases (Fig. 6) caused by complete natural carbonation are summarized in Table 4. As the free chloride concentration decreases, the loss in the physical binding ability increases. The losses at the free Cl^- concentrations of 0.05 mol/L, 0.40 mol/L, 0.67 mol/L, and 1.0 mol/L are 94.6%, 72.9%, 61.9% and 52.7%, respectively. This means that the physical binding behaviour is more susceptible to natural carbonation when cement-based materials suffer from a mild chloride attack.

When cement-based materials suffer from a mild chloride attack, AFm chemically reacts with chloride ions to produce Kuzel's salt [10]. Kuzel's salt may be converted into Friedel's salt during natural carbonation. However, complete natural carbonation can result in the dissolution of AFm, Kuzel's salt and Friedel's salt, as shown in Fig. 5. Therefore, the chemically bound chloride is released; and the completely carbonated cement-based materials are not capable of binding any chloride ions. This is similar to accelerated carbonation [48].

In practical engineering, RC structures are subjected to a combined attack by chloride and natural carbonation, particularly when they exposed to the coastal atmospheric environments. According to the results of the present study, the effects of the combined attack differ greatly from those of the accelerated carbonation in the laboratory, especially the effects of carbonation on the physical binding behaviours of chloride. The model based on Fick's second law is widely used for the durability design of RC structures. The results from the accelerated carbonation neglect the chloride binding capacity, which results in the overestimation of the chloride penetration depth and the free chloride concentration at the steel surface. Therefore, the durability design of RC structures based on the results of accelerated carbonation in the laboratory is conservative.

6. Conclusions

The effect of natural carbonation on chloride binding in OPC paste was investigated using a thermodynamic model, which was developed by using the experiment in Ref. [48] as the benchmark example. The phase assemblages, pH of the pore solution, physical and chemical binding capacities (i.e., the amounts of chloride bound by AFm and C–S–H), and the CBIs were predicted for cement-based materials subjected to different degrees of chloride attack and natural carbonation. The following conclusions are drawn:

(1) Complete natural carbonation of OPC paste leads to the disappearance of portlandite, ettringite and AFm phases, and a decrease in the Ca/Si ratio of C–S–H.

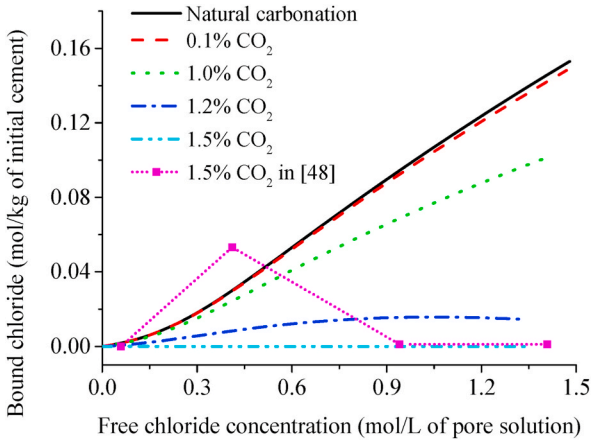

Fig. 7. Predicted chloride binding isotherms (CBIs) in the completely carbonated paste at different CO_2 concentrations.

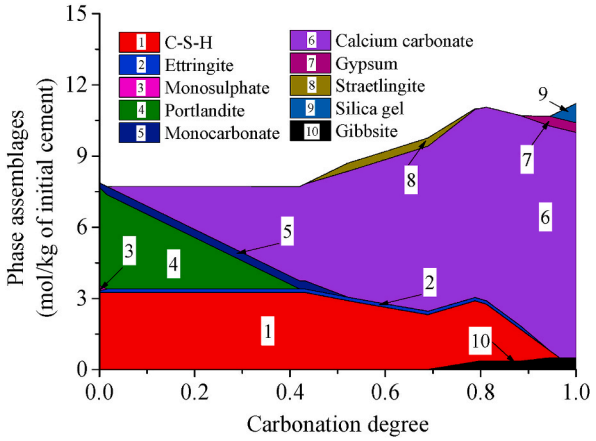

Fig. 8. Phase assemblages in the paste as a function of carbonation degree at 1.5% CO_2 concentration.

Table 4
Loss in the physical binding capacity for chloride in C–S–H.

Free Cl^- concentration (mol/L)	0.05	0.40	0.67	1.0
Loss in the physical binding capacity	94.6%	72.9%	61.9%	52.7%

(2) Kuzel's salt is produced when cement-based materials are exposed to a mild chloride attack. The Kuzel's salt can be converted to Friedel's salt during the natural carbonation process. As carbonation proceeds, the Friedel's salt disappears.
(3) Because natural carbonation cannot completely dissolve the C–S–H phase, the physical binding capacity is only partially lost even when cement-based materials undergo complete natural carbonation. The losses in the physical binding capacity in OPC paste at the free Cl^- concentrations of 0.05 mol/L, 0.40 mol/L, 0.67 mol/L and 1.0 mol/L are 94.6%, 72.9%, 61.9% and 52.7%, respectively. This differs from the complete loss of the chloride binding capacity in cement-based materials caused by accelerated carbonation. Therefore, the experimental results from the accelerated carbonation in the laboratory lead to a conservative durability design for the RC structures which are vulnerable to combined attack by chloride and carbonation.

Credit author statement

Bingbing Guo: Numerical simulation, Analysis, Writing-Original draft preparation, Funding acquisition. Guofu Qiao: Methodology, Writing-Review and Editing, Project administration, Funding acquisition. Peng Han: Methodology, Writing-Review and Editing. Zhenming Li: Conceptualization, Analysis, Methodology, Writing-Review and Editing. Qiang Fu: Methodology, Writing-Review and Editing.

Declaration of competing interest

The authors declare that they have no known competing financial interests or personal relationships that could have appeared to influence the work reported in this paper.

Acknowledgements

The authors are grateful for the financial support of the Nature Science Foundation of China (NSFC) (Project No.: 51908453 and 51578190), the National Key Research and Development Program of China (Project No.: 2018YFC0705606), the China Postdoctoral Science Foundation (Project No.: 2020M673607XB and 2020T130497), the Scientific Research of Shanxi Provincial Department of Education (Project No.: 20JK0710), the Independent Research and Development project of State Key Laboratory of Green Building in Western China (Project No.: LSZZ202113).

References

[1] U.M. Angst, Challenges and opportunities in corrosion of steel in concrete, Mater. Struct. 51 (2018) 4, https://doi.org/10.1617/s11527-017-1131-6.
[2] X. Shi, N. Xie, K. Fortune, J. Gong, Durability of steel reinforced concrete in chloride environments: an overview, Construct. Build. Mater. 30 (2012) 125–138, https://doi.org/10.1016/j.conbuildmat.2011.12.038.
[3] C.L. Page, K.W.J. Treadaway, Aspects of the electrochemistry of steel in concrete, Nature 297 (297) (1982) 109–1982.
[4] M. Stefanoni, U.M. Angst, B. Elsener, Kinetics of electrochemical dissolution of metals in porous media, Nat. Mater. 18 (9) (2019) 942–947, https://doi.org/10.1038/s41563-019-0439-8.
[5] U. Angst, B. Elsener, C.K. Larsen, Ø. Vennesland, Critical chloride content in reinforced concrete−A review, Cement Concr. Res. 39 (12) (2009) 1122–1138, https://doi.org/10.1016/j.cemconres.2009.08.006.
[6] U.M. Angst, B. Elsener, The size effect in corrosion greatly influences the predicted life span of concrete infrastructures, Sci. Adv. 3 (2017), e17007518, https://doi.org/10.1126/sciadv.1700751.
[7] G. Qiao, J. Ou, Corrosion monitoring of reinforcing steel in cement mortar by EIS and ENA, Electrochim. Acta 52 (28) (2007) 8008–8019, https://doi.org/10.1016/j.electacta.2007.06.070.
[8] Q. Liu, Z. Hu, X. Lu, J. Yang, I. Azim, W. Sun, Prediction of chloride distribution for offshore concrete based on statistical analysis, Materials 13 (1) (2020) 174, https://doi.org/10.3390/ma13010174.
[9] F.P. Glasser, A. Kindness, S.A. Stronach, Stability and solubility relationships in AFm phases: Part I. Chloride, sulfate and hydroxide, Cement Concr. Res. 29 (6) (1999) 861–866, https://doi.org/10.1016/S0008-8846(99)00055-1.
[10] A. Mesbah, M. François, C. Cau-dit-Coumes, F. Frizon, Y. Filinchuk, F. Leroux, J. Ravaux, G. Renaudin, Crystal structure of Kuzel's salt $3CaO{\cdot}Al_2O_3{\cdot}1/2CaSO_4{\cdot}1/2CaCl_2{\cdot}11H_2O$ determined by synchrotron powder diffraction, Cement Concr. Res. 41 (5) (2011) 504–509, https://doi.org/10.1016/j.cemconres.2011.01.015.
[11] A.K. Suryavanshi, J.D. Scantlebury, S.B. Lyon, Mechanism of Friedel's salt formation in cements rich in tri-calcium aluminate, Cement Concr. Res. 26 (5) (1996) 717–727, https://doi.org/10.1016/S0008-8846(96)85009-5.
[12] Y. Elakneswaran, T. Nawa, K. Kurumisawa, Electrokinetic potential of hydrated cement in relation to adsorption of chlorides, Cement Concr. Res. 39 (4) (2009) 340–344, https://doi.org/10.1016/j.cemconres.2009.01.006.
[13] Y. Elakneswaran, T. Nawa, K. Kurumisawa, Influence of surface charge on ingress of chloride ion in hardened pastes, Mater. Struct. 42 (2009) 83–93, https://doi.org/10.1617/s11527-008-9368-8.
[14] G. Plusquellec, A. Nonat, Interactions between calcium silicate hydrate (C-S-H) and calcium chloride, bromide and nitrate, Cement Concr. Res. 90 (2016) 89–96, https://doi.org/10.1016/j.cemconres.2016.08.002.
[15] I. Pointeau, P. Reiller, N. Macé, C. Landesman, N. Coreau, Measurement and modeling of the surface potential evolution of hydrated cement pastes as a function of degradation, J. Colloid Interface Sci. 300 (1) (2006) 33–44, https://doi.org/10.1016/j.jcis.2006.03.018.
[16] H. Hirao, K. Yamada, H. Takahashi, H. Zibara, Chloride binding of cement estimated by binding isotherms of hydrates, J. Adv. Concr. Technol. 1 (3) (2004) 77–84.
[17] G.K. Glass, N.R. Buenfeld, The influence of chloride binding on the chloride induced corrosion risk in reinforced concrete, Corrosion Sci. 42 (2) (2000) 329–344, https://doi.org/10.1016/S0010-938X(99)00083-9.
[18] B. Reddy, G.K. Glass, P.J. Lim, N.R. Buenfeld, On the corrosion risk presented by chloride bound in concrete, Cement Concr. Compos. 24 (1) (2002) 1–5, https://doi.org/10.1016/S0958-9465(01)00021-X.
[19] M.R. Jones, D.E. Macphee, J.A. Chudek, G. Hunter, R. Lannegrand, R. Talero, S.N. Scrimgeour, Studies using 27Al MAS NMR of AFm and AFt phases and the formation of Friedel's salt, Cement Concr. Res. 33 (2) (2003) 177–182, https://doi.org/10.1016/S0008-8846(02)00901-8.
[20] H. Friedmann, O. Amiri, A.A. T-Mokhtar, Physical modeling of the electrical double layer effects on multispecies ions transport in cement-based materials, Cement Concr. Res. 32 (2008) 1394–1400, https://doi.org/10.1016/j.cemconres.2008.06.003.
[21] G. Paul, E. Boccaleri, L. Buzzi, F. Canonico, D. Gastaldi, Friedel's salt formation in sulfoaluminate cements: a combined XRD and 27 Al MAS NMR study, Cement Concr. Res. 67 (2015) 93–102, https://doi.org/10.1016/j.cemconres.2014.08.004.
[22] Z. Hu, L. Mao, J. Xia, J. Liu, J. Gao, J. Yang, Q. Liu, Five-phase modelling for effective diffusion coefficient of chlorides in recycled concrete, Mag. Concr. Res. 70 (11) (2018) 583–594, https://doi.org/10.1680/jmacr.17.00194.
[23] Q. Liu, D. Easterbrook, L. Li, D. Li, Prediction of chloride diffusion coefficients using multi-phase models, Mag. Concr. Res. 69 (3) (2017) 134–144, https://doi.org/10.1680/jmacr.16.00134.
[24] L. Mao, Z. Hu, J. Xia, G. Feng, I. Azim, J. Yang, Q. Liu, Multi-phase modelling of electrochemical rehabilitation for ASR and chloride affected concrete composites, Compos. Struct. 207 (2019) 176–189, https://doi.org/10.1016/j.compstruct.2018.09.063.
[25] Q. Liu, D. Easterbrook, J. Yang, L. Li, A three-phase, multi-component ionic transport model for simulation of chloride penetration in concrete, Eng. Struct. 86 (2015) 122–133, https://doi.org/10.1016/j.engstruct.2014.12.043.
[26] Q. Liu, G. Feng, J. Xia, J. Yang, L. Li, Ionic transport features in concrete composites containing various shaped aggregates: a numerical study, Compos. Struct. 183 (SI) (2018) 371–380, https://doi.org/10.1016/j.compstruct.2017.03.088.
[27] H. Zibara, Binding of External Chloride by Cement Pastes, PhD Thesis, University of Toronto, Canada, 2001.
[28] X. Shen, W. Jiang, D. Hou, Z. Hu, J. Yang, Q. Liu, Numerical study of carbonation and its effect on chloride binding in concrete, Cement Concr. Compos. 104 (2019) 103402, https://doi.org/10.1016/j.cemconcomp.2019.103402.
[29] J. Liu, M. Ba, Y. Du, Z. He, J. Chen, Effects of chloride ions on carbonation rate of hardened cement paste by X-ray CT techniques, Construct. Build. Mater. 122 (2016) 619–627, https://doi.org/10.1016/j.conbuildmat.2016.06.101.
[30] V. Shah, K. Scrivener, B. Bhattacharjee, S. Bishnoi, Changes in microstructure characteristics of cement paste on carbonation, Cement Concr. Res. 109 (2018) 184–197, https://doi.org/10.1016/j.cemconres.2018.04.016.
[31] N. Seigneur, E. Kangni-Foli, V. Lagneau, A. Dauzères, S. Poyet, P.L. Bescop, E.L. Hôpital, J.B. D Espinose De Lacaillerie, Predicting the atmospheric carbonation of cementitious materials using fully coupled two-phase reactive transport modelling, Cement Concr. Res. 130 (2020) 105966, https://doi.org/10.1016/j.cemconres.2019.105966.
[32] B. Šavija, M. Luković, Carbonation of cement paste: understanding, challenges, and opportunities, Construct. Build. Mater. 117 (2016) 285–301, https://doi.org/10.1016/j.conbuildmat.2016.04.138.

[33] X. Liu, D. Niu, X. Li, Y. Lv, Effects of $Ca(OH)_2$ – $CaCO_3$ concentration distribution on the pH and pore structure in natural carbonated cover concrete: a case study, Construct. Build. Mater. 186 (2018) 1276–1285, https://doi.org/10.1016/j.conbuildmat.2018.08.041.
[34] A. Ueli, M. Fabrizio, G. Mette, K. Sylvia, B. Hans, Corrosion of steel in carbonated concrete: mechanisms, practical experience, and research priorities – a critical review by RILEM TC 281-CCC, RILEM Tech. Lett. (5) (2020) 85–100, https://doi.org/10.21809/rilemtechlett.2020.127.
[35] Intergovernmental Panel on Clima Change (IPCC), Climate Change 2013: the Physical Science Basis: Working Group I Contribution to the Fifth Assessment Report of the Intergovernmental Panel on Climate Change, Cambridge University Press, 2014.
[36] M.G. Stewart, X. Wang, M.N. Nguyen, Climate change adaptation for corrosion control of concrete infrastructure, Struct. Saf. 35 (2012) 29–39, https://doi.org/10.1016/j.strusafe.2011.10.002.
[37] A. Leemann, F. Moro, Carbonation of concrete: the role of CO_2 concentration, relative humidity and CO_2 buffer capacity, Mater. Struct. 50 (1) (2017) 1–14, https://doi.org/10.1617/s11527-016-0917-2.
[38] A. Leemann, P. Nygaard, J. Kaufmann, R. Loser, Relation between carbonation resistance, mix design and exposure of mortar and concrete, Cement Concr. Compos. 62 (2015) 33–43, https://doi.org/10.1016/j.cemconcomp.2015.04.020.
[39] S. Goni, A. Guerrero, Accelerated carbonation of Friedel's salt in calcium aluminate cement paste, Cement Concr. Res. 33 (2003) 21–26, https://doi.org/10.1016/S0008-8846(02)00910-9.
[40] A.K. Suryavanshi, R.N. Swamy, Stability of Friedel's salt in carbonated concrete structural elements, Cement Concr. Res. 26 (5) (1996) 729–741, https://doi.org/10.1016/S0008-8846(96)85010-1.
[41] J. Geng, D. Easterbrook, Q. Liu, L. Li, Effect of carbonation on release of bound chlorides in chloride-contaminated concrete, Mag. Concr. Res. 68 (7) (2016) 353–363, https://doi.org/10.1680/jmacr.15.00234.
[42] P. Chindaprasirt, S. Rukzon, V. Sirivivatnanon, Effect of carbon dioxide on chloride penetration and chloride ion diffusion coefficient of blended Portland cement mortar, Construct. Build. Mater. 22 (8) (2008) 1701–1707, https://doi.org/10.1016/j.conbuildmat.2007.06.002.
[43] J. Liu, Q. Qiu, X. Chen, F. Xing, N. Han, Y. He, Y. Ma, Understanding the interacted mechanism between carbonation and chloride aerosol attack in ordinary Portland cement concrete, Cement Concr. Res. 95 (2017) 217–225, https://doi.org/10.1016/j.cemconres.2017.02.032.
[44] H. Ye, X. Jin, C. Fu, N. Jin, Y. Xu, T. Huang, Chloride penetration in concrete exposed to cyclic drying-wetting and carbonation, Construct. Build. Mater. 112 (2016) 457–463, https://doi.org/10.1016/j.conbuildmat.2016.02.194.
[45] H. Kuosa, R.M. Ferreira, E. Holt, M. Leivo, E. Vesikari, Effect of coupled deterioration by freeze–thaw, carbonation and chlorides on concrete service life, Cement Concr. Compos. 47 (2014) 32–40, https://doi.org/10.1016/j.cemconcomp.2013.10.008.
[46] J. Backus, D. McPolin, M. Basheer, A. Long, N. Holmes, Exposure of mortars to cyclic chloride ingress and carbonation, Adv. Cement Res. 25 (1) (2013) 3–11, https://doi.org/10.1680/adcr.12.00029.
[47] H. Chang, Chloride binding capacity of pastes influenced by carbonation under three conditions, Cement Concr. Compos. 84 (2017) 1–9, https://doi.org/10.1016/j.cemconcomp.2017.08.011.
[48] M. Saillio, V. Baroghel-Bouny, F. Barberon, Chloride binding in sound and carbonated cementitious materials with various types of binder, Construct. Build. Mater. 68 (2014) 82–91, https://doi.org/10.1016/j.conbuildmat.2014.05.049.
[49] X. Zhu, G. Zi, Z. Cao, X. Cheng, Combined effect of carbonation and chloride ingress in concrete, Construct. Build. Mater. 110 (2016) 369–380, https://doi.org/10.1016/j.conbuildmat.2016.02.034.
[50] M. Castellote, L. Fernandez, C. Andrade, C. Alonso, Chemical changes and phase analysis of OPC pastes carbonated at different CO_2 concentrations, Mater. Struct. 42 (4) (2009) 515–525, https://doi.org/10.1617/s11527-008-9399-1.
[51] G.W. Groves, A. Brough, I.G. Richardson, C.M. Dobson, Progressive changes in the structure of hardened C_3S cement pastes due to carbonation, J. Am. Ceram. Soc. 74 (11) (1991) 2891–2896, https://doi.org/10.1111/j.1151-2916.1991.tb06859.x.
[52] D.J. Anstice, C.L. Pageb, M.M. Page, The pore solution phase of carbonated cement pastes, Cement Concr. Res. 35 (2005) 377–383, https://doi.org/10.1016/j.cemconres.2004.06.041.
[53] N. Hyvert, A. Sellier, F. Duprat, P. Rougeau, P. Francisco, Dependency of C–S–H carbonation rate on CO_2 pressure to explain transition from accelerated tests to natural carbonation, Cement Concr. Res. 40 (2010) 1582–1589.
[54] B. Lothenbach, D.A. Kulik, T. Matschei, M. Balonis, L. Baquerizo, B. Dilnesa, G.D. Miron, R.J. Myers, Cemdata 18: a chemical thermodynamic database for hydrated Portland cements and alkali-activated materials, Cement Concr. Res. 115 (2019) 472–506, https://doi.org/10.1016/j.cemconres.2018.04.018.
[55] B. Lothenbach, F. Winnefeld, Thermodynamic modelling of the hydration of Portland cement, Cement Concr. Res. 36 (2) (2006) 209–226, https://doi.org/10.1016/j.cemconres.2005.03.001.
[56] B. Lothenbach, Thermodynamic equilibrium calculations in cementitious systems, Mater. Struct. 43 (10) (2010) 1413–1433, https://doi.org/10.1617/s11527-010-9592-x.
[57] B. Lothenbach, T. Matschei, G. Möschner, F.P. Glasser, Thermodynamic modelling of the effect of temperature on the hydration and porosity of Portland cement, Cement Concr. Res. 38 (1) (2008) 1–18, https://doi.org/10.1016/j.cemconres.2007.08.017.
[58] B. Lothenbach, M. Zajac, Application of thermodynamic modelling to hydrated cements, Cement Concr. Res. 105779 (13) (2019).
[59] Y. Elakneswaran, A. Iwasa, T. Nawa, T. Sato, K. Kurumisawa, Ion-cement hydrate interactions govern multi-ionic transport model for cementitious materials, Cement Concr. Res. 40 (12) (2010) 1756–1765, https://doi.org/10.1016/j.cemconres.2010.08.019.
[60] F.P. Glasser, J. Marchand, E. Samson, Durability of concrete — degradation phenomena involving detrimental chemical reactions, Cement Concr. Res. 38 (2) (2008) 226–246, https://doi.org/10.1016/j.cemconres.2007.09.015.
[61] T. Van Quan, A. Soive, S. Bonnet, A. Khelidj, A numerical model including thermodynamic equilibrium, kinetic control and surface complexation in order to explain cation type effect on chloride binding capability of concrete, Construct. Build. Mater. 191 (2018) 608–618, https://doi.org/10.1016/j.conbuildmat.2018.10.058.
[62] B. Guo, Y. Hong, G. Qiao, J. Ou, A COMSOL-PHREEQC interface for modeling the multi-species transport of saturated cement-based materials, Construct. Build. Mater. 187 (2018) 839–853, https://doi.org/10.1016/j.conbuildmat.2018.07.242.
[63] W.M. Haynes, D.R. Lide, T.J. Bruno, CRC Handbook of Chemistry and Physics, CRC Press, 2014.
[64] V.Q. Tran, A. Soive, V. Baroghel-Bouny, Modelisation of chloride reactive transport in concrete including thermodynamic equilibrium, kinetic control and surface complexation, Cement Concr. Res. 110 (2018) 70–85, https://doi.org/10.1016/j.cemconres.2018.05.007.
[65] D.A. Kulik, Improving the structural consistency of C-S-H solid solution thermodynamic models, Cement Concr. Res. 41 (5) (2011) 477–495, https://doi.org/10.1016/j.cemconres.2011.01.012.
[66] I.G. Richardson, Tobermorite/jennite- and tobermorite/calcium hydroxide-based models for the structure of C-S-H: applicability to hardened pastes of tricalcium silicate, β-dicalcium silicate, Portland cement, and blends of Portland cement with blast-furnace slag, metakaolin, or silica fume, Cement Concr. Res. 34 (9) (2004) 1733–1777, https://doi.org/10.1016/j.cemconres.2004.05.034.
[67] D.L. Parkhurst, C.A.J. Appelo, Description of Input and Examples for PHREEQC Version 3—A Computer Program for Speciation, Batch-Reaction, One-Dimensional Transport, and Inverse Geochemical Calculations, U.S. Geological Survey, 2013.
[68] S.R. Charlton, D.L. Parkhurst, Modules based on the geochemical model PHREEQC for use in scripting and programming languages, Comput. Geosci.-UK. 37 (10) (2011) 1653–1663, https://doi.org/10.1016/j.cageo.2011.02.005.
[69] H. Viallis-Terrisse, A. Nonat, J. Petit, Zeta-Potential study of calcium silicate hydrates interacting with alkaline cations, J. Colloid Interface Sci. 244 (1) (2001) 58–65, https://doi.org/10.1006/jcis.2001.7897.
[70] B. Guo, Y. Hong, G. Qiao, J. Ou, Z. Li, Thermodynamic modeling of the essential physicochemical interactions between the pore solution and the cement hydrates in chloride-contaminated cement-based materials, J. Colloid Interface Sci. 531 (2018) 56–63, https://doi.org/10.1016/j.jcis.2018.07.005.
[71] M.V.A. Florea, H.J.H. Brouwers, Chloride binding related to hydration products Part I: ordinary Portland Cement, Cement Concr. Res. 42 (2) (2012) 282–290, https://doi.org/10.1016/j.cemconres.2011.09.016.

[72] M. Balonis, B. Lothenbach, G. Le Saout, F.P. Glasser, Impact of chloride on the mineralogy of hydrated Portland cement systems, Cement Concr. Res. 40 (2010) 1009–1022, https://doi.org/10.1016/j.cemconres.2010.03.002.
[73] M.D.A. Thomas, R.D. Hooton, A. Scott, H. Zibara, The effect of supplementary cementitious materials on chloride binding in hardened cement paste, Cement Concr. Res. 42 (1) (2012) 1–7, https://doi.org/10.1016/j.cemconres.2011.01.001.
[74] S. von Greve-Dierfeld, B. Lothenbach, A. Vollpracht, B. Wu, B. Huet, C. Andrade, C. Medina, C. Thiel, E. Gruyaert, H. Vanoutrive, I.F. Saéz Del Bosque, I. Ignjatovic, J. Elsen, J.L. Provis, K. Scrivener, K. Thienel, K. Sideris, M. Zajac, N. Alderete, Ö. Cizer, P. Van den Heede, R.D. Hooton, S. Kamali-Bernard, S. A. Bernal, Z. Zhao, Z. Shi, N. De Belie, Understanding the carbonation of concrete with supplementary cementitious materials: a critical review by RILEM TC 281-CCC, Mater. Struct. 53 (6) (2020), https://doi.org/10.1617/s11527-020-01558-w.
[75] Z. Shi, B. Lothenbach, M.R. Geiker, J. Kaufmann, A. Leemann, S. Ferreiro, J. Skibsted, Experimental studies and thermodynamic modeling of the carbonation of Portland cement, metakaolin and limestone mortars, Cement Concr. Res. 88 (2016) 60–72, https://doi.org/10.1016/j.cemconres.2016.06.006.
[76] H. Chang, P. Feng, K. Lyu, J. Liu, A novel method for assessing C-S-H chloride adsorption in cement pastes, Construct. Build. Mater. 225 (2019) 324–331, https://doi.org/10.1016/j.conbuildmat.2019.07.212.